

# The Effect of Rain and Water Vapor on Sky Noise at Centimeter Wavelengths

By D. C. HOGG and R. A. SEMPLAK

(Manuscript received March 7, 1961)

*Measurements of sky noise temperature at a frequency of 6.0 kmc have been made for various conditions of absolute humidity and precipitation. For an antenna beam position  $5^\circ$  above the horizon, the sky noise temperature was found to increase about  $15^\circ\text{K}$  from winter to summer due to the change in absolute humidity. During periods of rain, with the antenna beam pointed to the zenith, sky noise temperatures as high as  $130^\circ\text{K}$  have been observed, compared with the usual background value of  $3^\circ$  due to oxygen and water vapor. Theoretical calculations of sky noise temperature for typical dry and humid summer days are presented.*

## I. INTRODUCTION

This study is directed toward evaluating the variability in the noise level of sensitive ground-based microwave receivers to be used in radar or space communications.<sup>1</sup> The sensitivity of such receivers is limited by the antenna noise received from the sky due to emission of radiation by the earth's atmosphere and by noise sources in space. The sun and moon and the galaxy are serious noise contributors in space; however, since the sun and moon are seldom in the antenna beam and since galaxy noise is small at centimeter wavelengths, sky noise is due mainly to emission by the earth's atmosphere. The atmosphere contains oxygen and water vapor, both of which absorb and therefore emit radio waves, especially in the microwave band. The oxygen content is relatively constant in time; it therefore produces a sensibly constant background noise. However, the water vapor content and the noise it produces change with location and season. Condensed water, in the form of rain, is a strong absorber of microwaves and contributes a significant amount of noise, whose level changes with time.

A brief theoretical treatment outlining the amount of noise to be

expected from the atmosphere is followed by a discussion of experimental data obtained at a frequency of 6 kmc from a receiving site, at an elevation of 370 feet above sea level, located at Crawford Hill, Holmdel, New Jersey.

## II. THEORETICAL DISCUSSION

The noise received from a horizontally stratified atmosphere by the infinitely sharp beam of an idealized antenna is given by  $P_a = kT_s B$ , where  $k$  is Boltzmann's constant,  $B$  is bandwidth, and  $T_s$  is effective sky temperature. If there is no precipitation, oxygen and water vapor are the two most significant contributors of noise, and the sky noise temperature is

$$T_s = \int_0^\infty (\alpha_1 + \alpha_2) T \exp \left[ - \int_0^r (\alpha_1 + \alpha_2) dr \right] dr, \quad (1)$$

with  $T$  being the actual temperature at a given point  $P$  in the atmosphere defined by the distance  $r$  along the antenna beam and an angle  $\varphi$ , as shown in Fig. 1;  $\alpha_1$  is the power absorption coefficient due to oxygen at point  $P$  and  $\alpha_2$  is that due to water vapor, both being functions of frequency, temperature, and pressure. The oxygen absorption coefficient  $\alpha_1$  is due to the magnetic dipole resonance of the oxygen molecule at frequencies near 60 kmc. Pressure-broadening causes the skirts of these resonance lines to extend through the centimeter wave region, and the absorption contributes significantly to antenna noise. The water vapor absorption coefficient  $\alpha_2$  consists of two terms, absorption due to the electric dipole resonance of the water molecule near 22.5 kmc and that due to the skirts of rotational lines in the infrared region.

Assuming a perfectly dry atmosphere,  $\alpha_2 = 0$ , and the effective sky noise temperature due to oxygen alone can be calculated using (1). These values are plotted as the lower curves of the groups of curves shown in Fig. 2; they are based upon the temperature and pressure dependence of Fig. 1(a). The four sets of curves in Fig. 2 correspond to various beam directions,  $\phi$ , of the antenna. The central curves in the figures are also calculated for standard temperature and pressure conditions, but in this case,  $\alpha_2$  is not zero\* since the atmosphere is assumed to contain water

\* In these calculations a line-broadening constant of  $0.3 \text{ cm}^{-1}$  is used for the infrared lines; this choice is based on absorption measurements in the millimeter wavelength region. It has recently been proposed<sup>3</sup> that mutual coupling between  $\text{O}_2$  and  $\text{H}_2\text{O}$  molecules in air may cause additional absorption at millimeter wavelengths and that the broadening constant should be  $0.1 \text{ cm}^{-1}$ , as it is for the 22.5 kmc line. This value would decrease considerably the noise temperature due to water vapor in the calculated curves of Fig. 2. Nevertheless, the measured data indicated in Fig. 6 appear to justify the use of  $0.3 \text{ cm}^{-1}$  as the line-broadening constant.

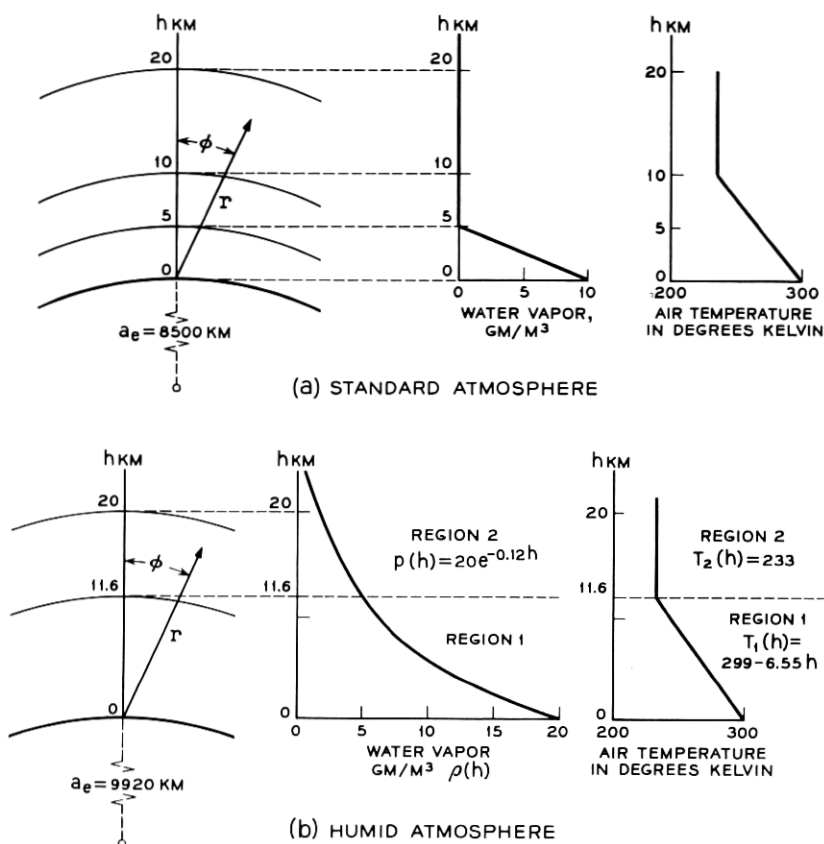


Fig. 1 — (a) Assumed model of standard summer atmosphere; (b) model of very humid summer atmosphere based on meteorological data from Newark Air Service.

vapor of density 10 grams per cubic meter at the surface of the earth, which decreases linearly to zero at an altitude of 5 kilometers, as shown in Fig. 1(a). This condition is representative of average summer conditions in temperate zones. In computing both the lower and central curves, the standard value  $\frac{4}{3}$  was used for the normalized radio radius of the earth.

The upper curves in Fig. 2 were calculated for an atmosphere of a typical humid summer day. This model atmosphere, shown in Fig. 1(b), is based upon meteorological data for August 8, 1960.\* The normalized radio radius calculated from these data is  $\frac{3}{2}$  rather than  $\frac{4}{3}$ , which means

\* Measured by the Newark Air Service at Newark Airport, Newark, New Jersey.

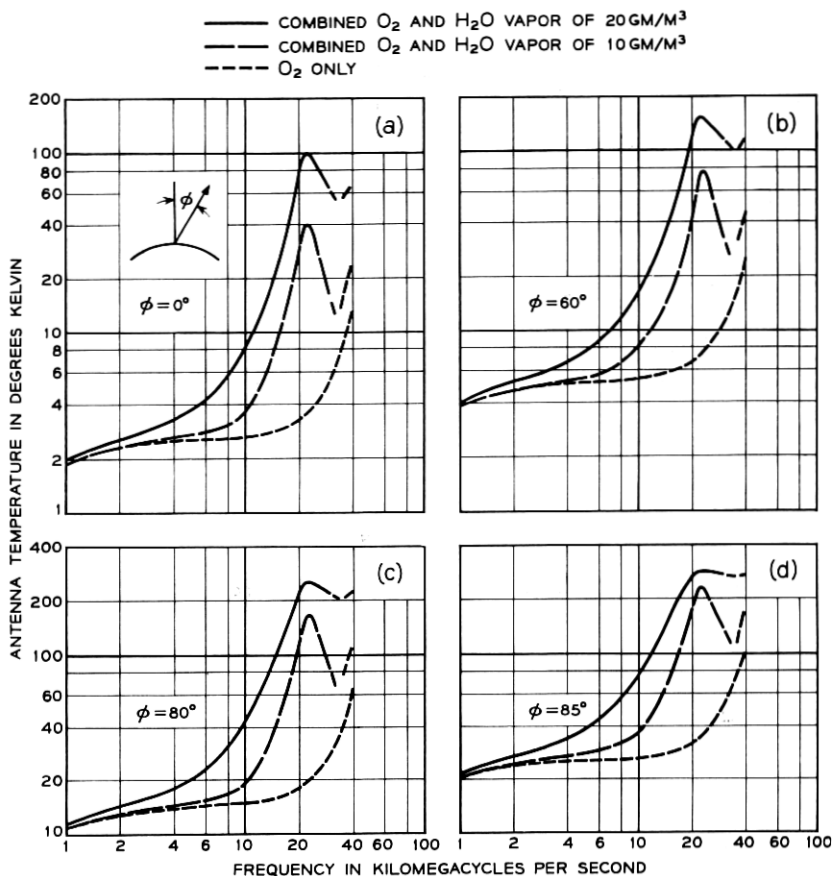


Fig. 2 — Typical sky noise temperatures for various antenna positions. In each case, lower curve is for very dry weather, center curve for average weather, and upper curve for very humid weather.

that for large values of  $\phi$  the antenna beam has a much longer path length through this atmosphere than through the one discussed above. This earth radius and the data of Fig. 1(b) were used in (1) to compute the upper curves of Fig. 2. Because of the rather extreme models chosen for the atmospheres upon which the upper and lower curves are based, they, in the absence of super-refraction and condensation, represent upper and lower bounds on the sky noise one may expect from the atmosphere in the microwave band.

Calculation of the effect of rain on sky noise temperature is difficult, in spite of the fact that the theoretical power absorption coefficient<sup>4</sup> is

known to agree well with measurements of absorption by rain in the microwave band. Difficulty arises because condensed water in the atmosphere is not horizontally stratified. Moreover, the distribution of condensed water as a function of altitude varies considerably with meteorological conditions. For example, weather radar measurements have shown that rain may originate as high as 45,000 feet.\* However, if the distribution of water along the path of the antenna beam were known, neglecting scattering by the raindrops, one would obtain its effect on noise temperature from (1) by substituting for  $\alpha_1 + \alpha_2$  the appropriate  $\alpha(r)$  for the water distribution. Thus, a measurement of sky noise is an integrated measure of the water content in the antenna beam.

### III. APPARATUS

For measurement of sky noise, it is desirable that the antenna and receiver proper have low intrinsic noise, relatively large bandwidth, and good stability. If these conditions are met, accurate absolute values of sky noise can be obtained and rapid changes in the level can be observed. A receiving system<sup>5</sup> that meets these requirements consists of a traveling-wave maser<sup>6</sup> and a horn-reflector antenna.

This type of antenna was designed for microwave radio relay systems and is shown in Fig. 3; it consists of a section of a paraboloid fed by a pyramidal horn. The antenna is broadband and is well matched. However, its virtues as a low-noise antenna stem from the fact that the far side and rear lobes are about 30 db below the isotropic level, thus allowing only a small amount of noise from the earth (which is a good absorber at microwaves) to enter the antenna; also, only a short length of transmission line is required between the horn and receiver proper (0.1 db transmission loss at room temperature produces  $7\frac{1}{2}^\circ\text{K}$  of noise). At 6 kmc, the beamwidth of the antenna shown in Fig. 3 is about 1.75 degrees and its gain is 40 db. The antenna mount permits movement in the elevation plane only, but in this plane the antenna beam may be moved from horizon to horizon. To permit this movement, a rotary joint is used in the waveguide run between the antenna and the maser. The length of this waveguide run is minimized to reduce waveguide losses and their associated noise contributions. A means of ensuring the rapid exit of water from the antenna is of practical concern, since the aperture is open to the elements; a few holes in the seam formed by the parabolic section and horn satisfy this requirement.

The essential features of the receiver proper are shown in Fig. 4 in

\* Private communication through the courtesy of J. S. Marshall, McGill University, Montreal, Canada.

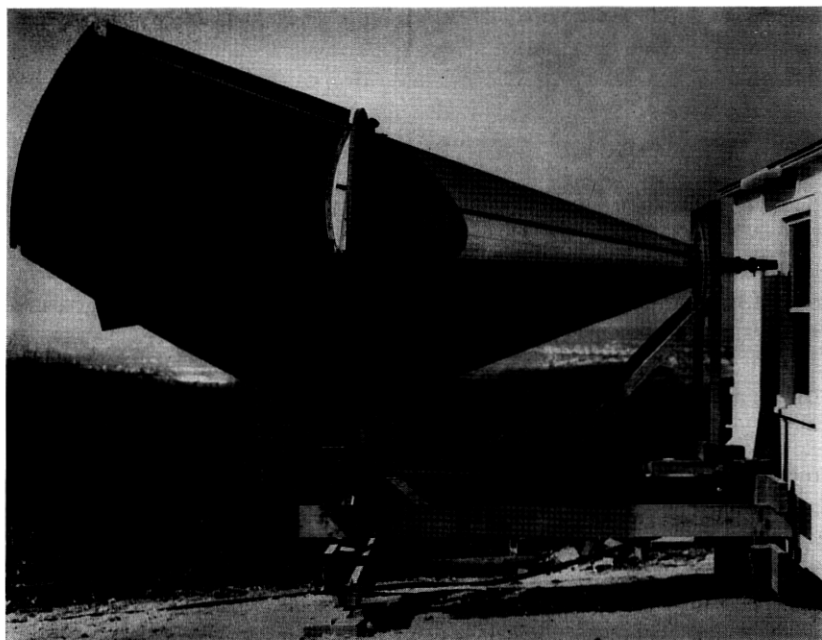


Fig. 3 — Horn-reflector antenna.

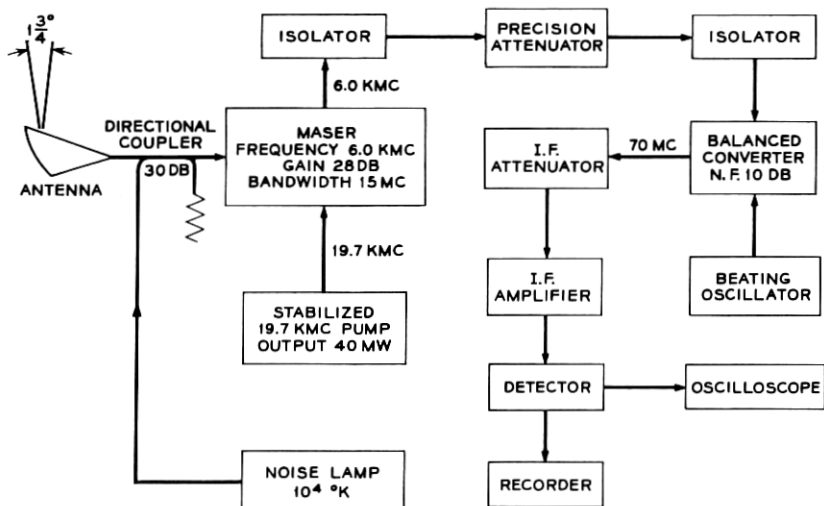


Fig. 4 — Low-noise receiver for 6 kmc.

block diagram form. At 6 kmc, the traveling-wave maser has a gain of 28 db and a bandwidth of 15 mc at a liquid helium temperature of 1.5°K. The magnetic field for the maser is provided by a permanent magnet. The pumping power is obtained from a stabilized 19.7-kmc klystron with an output of approximately 40 mw. Isolators are used between maser and attenuator and between attenuator and balanced converter to prevent the possibility of noise power re-entering the maser and, due to any input mismatch, reappearing as a net increase in input temperature. The remainder of the system utilizes a balanced crystal converter and IF amplification.

#### IV. MEASUREMENT TECHNIQUES

The over-all input noise temperature of the receiver consists of a constant term, which includes noise due to the antenna, input waveguide loss, maser, and the contribution from the second stage; these amount to 15.5°K, which is the limit of the sensitivity of the receiver proper. An additional term is the sky noise temperature, which varies as a function of the microwave absorption in the volume of the sky subtended by the antenna beam; on a clear day the sky noise is about 3°K, which increases the input noise to 18.5°K.

During periods of relatively stable atmospheric conditions a comparison method employing an argon noise lamp is used to measure the input temperature. The noise lamp is coupled into the input waveguide through a 30-db directional coupler. With the noise lamp switched off, the room temperature load which terminates the noise lamp introduces about 0.3°K; when the noise lamp is fired, the input noise is increased by 10°K. The change in noise level is determined by using a precision microwave attenuator. This is set at zero with the noise lamp off, and the IF gain of the measuring equipment is adjusted to obtain a suitable output level of detected noise; then the noise lamp is fired, and the precision attenuator is adjusted to give the same noise output from the measuring set.

The noise temperature at the input to the converter,  $T_{ic}$ , with the noise lamp off, is given by

$$T_{ic} = G_m(T_a + T_m), \quad (2)$$

where

$G_m$  is the gain of the maser,

$T_a$  is the effective antenna noise temperature (waveguide, antenna, and sky), and

$T_m$  is the effective noise temperature of the maser.

In this equation a small noise due to losses between maser and converter has been neglected. When the noise lamp is fired, the noise input to the converter becomes

$$T_{ic} = (T_a + T_m + T_L)G_m A + (1 - A)T_0, \quad (3)$$

where

$T_L$  is the additional noise introduced into the input waveguide by the noise lamp,

$T_0$  is ambient room temperature, and

$A$  is the reciprocal of the additional attenuation introduced by the precision attenuator.

Let  $T_i = T_a + T_m$ ; then, solving (2) and (3),

$$T_i = \frac{AT_L}{1 - A} + \frac{T_0}{G_m}.$$

The second term of this equation is the noise contribution of the precision attenuator; with maser gains in the order of 30 db, it is less than 0.5°K.

The noise-lamp method of measurement, although quite accurate, is time-consuming and does not lend itself readily to continuous measurement, since atmospheric conditions can and do change rapidly. For a continuous record of the changes in sky noise, the detected output of the intermediate frequency amplifier is applied to a two-channel Sanborn recorder. On one channel the full-scale sensitivity is of the order of 250°K, while on the second channel it is  $\pm 6^\circ\text{K}$ . It should be noted that a 15-mc band is preserved up to the recorder and that the recorder has a maximum bandwidth of 80 cps. Simultaneously, the output is displayed on an oscilloscope.

Ground-rain rate data obtained from a calibrated tipping-bucket rain gauge located about 50 feet from the antenna are fed to a timing channel on the recorder; each tip of the rain gauge bucket indicates that 0.01 inch of rain has fallen. This type of gauge is fairly accurate, provided the wind is not excessive. The time interval between two consecutive bucket tips is carefully measured, and the rainfall rate is then plotted at the mean value of time of two consecutive tips. This procedure was used for all recorded bucket tips.

## V. DISCUSSION OF MEASURED DATA

### 5.1. *The Water Vapor Effect*

Fig. 5 shows a set of data taken on October 7, 1960, with sky temperature plotted as ordinate and antenna beam position as abscissa. This



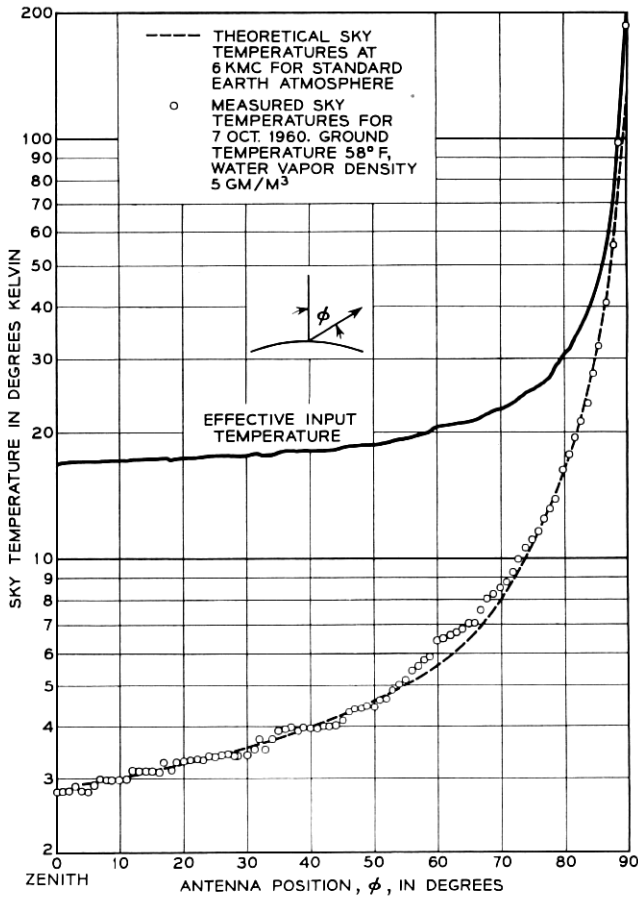


Fig. 5 — Sky noise temperature for a dry clear day.

particular day was dry and clear; based on temperature and humidity measurements made at the receiving site, the absolute water vapor density was 5 grams per cubic meter at the ground. The curve labeled "effective input temperature" shows the values of the first-circuit input noise temperature for various antenna positions; these values are the sum of the sky temperature plus the noise temperature contributed by input waveguide losses, maser noise, and antenna. The actual sky temperatures for the various antenna beam positions are plotted as dots. These data were obtained by averaging groups of measurements taken for each antenna beam position, as the antenna was moved from zenith to horizon in one-degree increments. For comparison, the dashed curve

represents the theoretical sky temperature based on a standard earth's atmosphere, as obtained from the central curves of Fig. 2.

From the relative smoothness of the dotted curve in Fig. 5 and the absence of abrupt changes, one concludes that the back and side lobes of the antenna allow only a small amount of noise radiation from the earth into the system. There is little difference in sky noise between that measured for a water vapor density of 5 grams per cubic meter and the theoretical values based on a water vapor density of 10 grams per cubic meter. A period of two and one-half hours was required to complete this set of measurements. During this time atmospheric conditions could have changed somewhat, even though no change was visibly detectible.

In order to determine the effects of water vapor density, antenna temperatures were measured for various sky conditions at random times during the year 1959-60. Fig. 6 shows the increase in sky temperature above zenith temperature for various water vapor densities. Again, the values for water vapor density were based on measurements made at the receiving site. Measurements with the antenna beamed  $60^\circ$ ,  $85^\circ$ , and  $87\frac{1}{2}^\circ$  from the zenith are shown. As the antenna beam approaches the horizon, it looks through greater amounts of the earth's atmosphere, so that the water vapor effect is accentuated. The data show more or less what we might expect: the noise temperatures increase with increasing water vapor density. The data shown here are conservative because they are taken relative to the zenith temperature for the day that the measurements were made; in other words, if this were not done, the slope of the curves would be slightly greater. With the antenna beam at  $60^\circ$  from the zenith, the sky noise temperature increases about  $1^\circ$  from winter to summer; at  $85^\circ$  from zenith, it increases  $15^\circ$  from winter to summer. These increases are partly due to changes in the effective radius of the earth, since the refractive index profile also changes with water vapor content. The scatter in the data is partly due to the following: water vapor measurements are only made at the receiving site; the distribution of water vapor with height is unknown, and hence the changes in the effective earth's radius are also unknown.

The dashed curves in Fig. 6 connect three theoretical noise temperatures for water vapor contents 0, 10, and 20 grams per cubic meter, as obtained from Fig. 2. Especially in the case of the  $85^\circ$  curve, agreement with the experimental data is considered to be good.

### 5.2 *The Rain Effect*

Sky temperature measurements taken on a drizzly day (May 18, 1960) for various zenith angles of the antenna beam are shown in Fig. 7; the

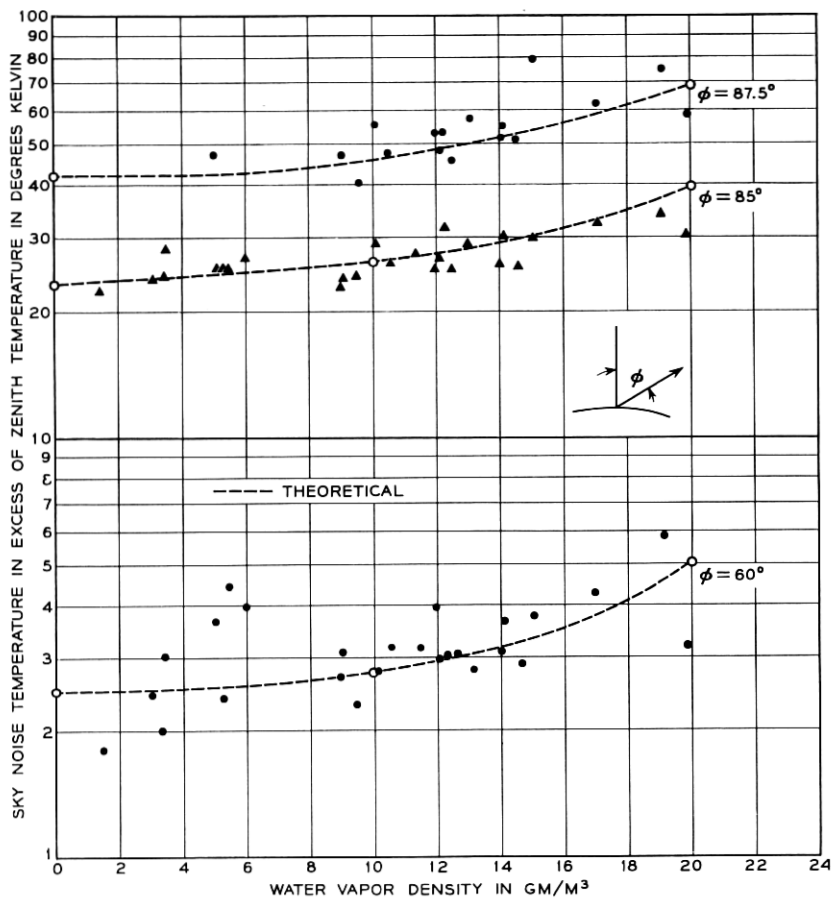


Fig. 6 — The effect of water vapor on sky noise temperature.

ground rain rate of about 6 millimeters per hour is also indicated on the figure.\* The increase in sky temperature due to the light rain is readily apparent. The curve titled "18 May 1960 2:45 p.m." in this group is interesting, for here, at beam position of  $85^\circ$  and greater, the noise temperature is essentially the same as it is for the dry day. Hence it appears as though the rain was fairly local at the time the measurements were made. All data discussed so far were obtained using the RF attenuator method.

\* It should be emphasized that the indicated rainfall rates are measured at the antenna site. When the beam approaches the horizon, however, it looks through several hundred miles of atmosphere, which may contain rain of various densities. In this case, the measured rain rate at the receiving site is of little significance.

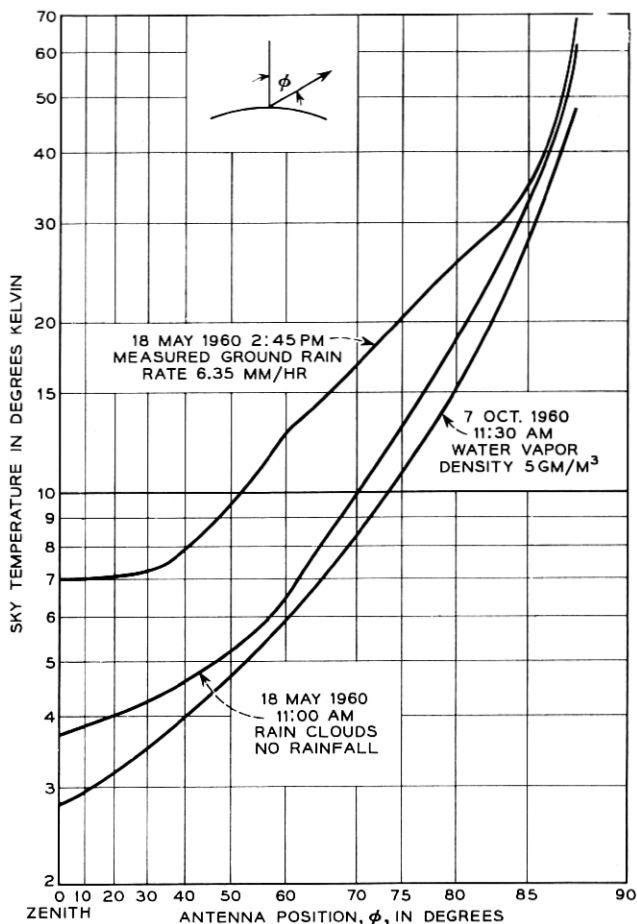


Fig. 7 — Sky noise temperatures for dry and wet days.

Sky temperature data for rapidly changing sky conditions which occur during periods of rainfall, obtained by means of the recorder, are shown in Figs. 8 through 12. These were selected as representative of the changes which usually occur in zenith sky temperature just prior to and on arrival of the rain at the ground. The left ordinate is zenith sky temperature, the right ordinate ground rain rate, with time on the abscissa. Before the arrival of the rain and after its departure from the location, the sky temperature may undergo variations on the order of several degrees. One should note on the measured data that an abrupt increase in sky noise is observed well before any significant rain is measured at

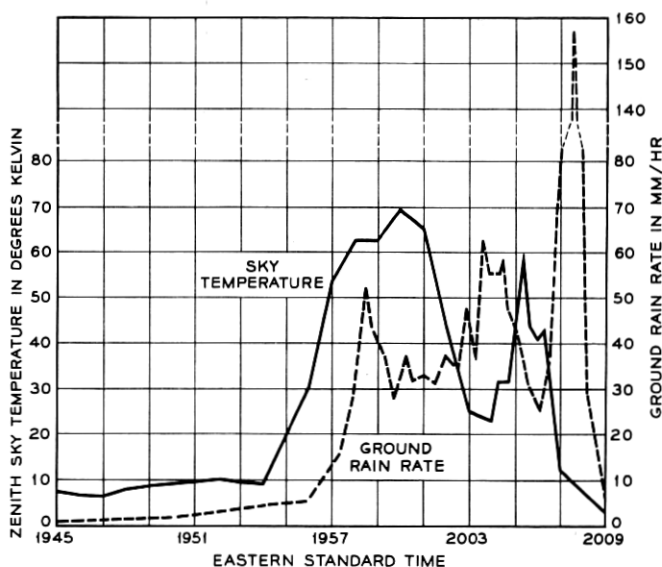


Fig. 8 — Sky noise temperatures observed during a rain storm (June 24, 1960); note that the sky temperature increases before the rain rate.

the ground; hence the sky noise is a precursor of rain at the ground. Most probably, the precursory action is due to a slope in the rain column as the water falls from a fairly localized cloud which is moving with the upper wind.\* Thus the antenna beam sees a maximum water density before it is observed at the ground.

Of special interest are the data shown in the last portion of Fig. 9

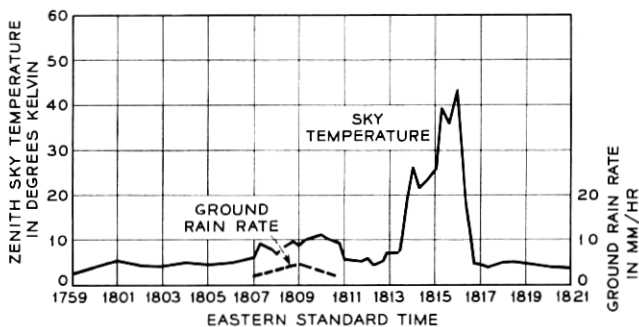


Fig. 9 — Relatively high sky noise with little or no measurable rainfall (June 24, 1960).

\* See Fig. 9 of Ref. 7.

Note that, although the sky temperature increased more than  $40^{\circ}\text{K}$ , no rain was recorded. It is apparent here that the antenna beam looked through a cloud containing a large amount of condensed water. Even though no rainfall was recorded at the receiving site, the water from this cloud was no doubt released further along the path of the storm. The data in Fig. 9 are in direct contrast with those in the last portion of Fig. 8, for in the latter case a rain rate in excess of 150 millimeters per hour produced only moderate sky temperatures. A good example of the rapid and large changes that can occur in sky temperature is shown in Fig. 10: in a period of about 40 seconds it increased  $66^{\circ}\text{K}$ . The abrupt break in the sky temperature curve was due to a 20-second power interruption caused by lightning; the remainder of the interval was used in re-checking the calibration of the measuring equipment.

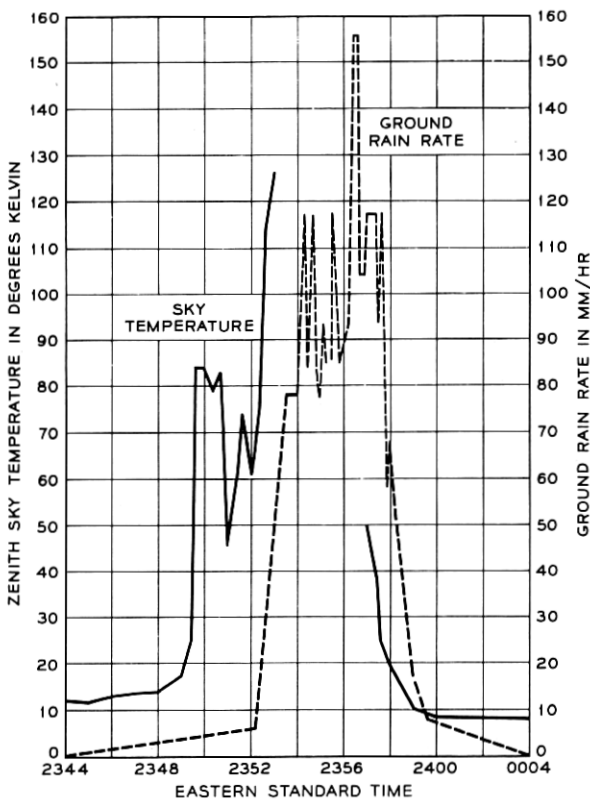


Fig. 10 — Data obtained during a severe thunderstorm (June 17, 1960).

There appears to be no detailed correlation between measured ground rain rate and zenith sky temperature; for example, in Fig. 11, fairly high sky temperatures were recorded when ground rain rates were low. This lack of correlation is further indicated in Fig. 12(a), for during the period shown the noise is fairly high but no measurable amount of rain fell. Fig. 12(b), however, shows that small variations in zenith temperature can occur with correspondingly low rain rates. Since data of this type are a measure of the water content of the atmosphere, they are of some meteorological significance and perhaps may serve as adjuncts to measurements by weather radar.

Since rain noise in space receivers plays the counterpart of signal fading in line-of-sight communications, a percentage-time distribution of sky noise is required for making reliability estimates. Although a relatively small statistical sample has been obtained so far, Fig. 13 shows both distributions of zenith sky noise temperature and ground rain rates. Additional measurements at the zenith and especially at beam positions near the horizon, where the background noise is higher, are needed to improve the statistics and to indicate the limit for a communication system. The median value of zenith sky temperature is  $14.7^{\circ}\text{K}$  or

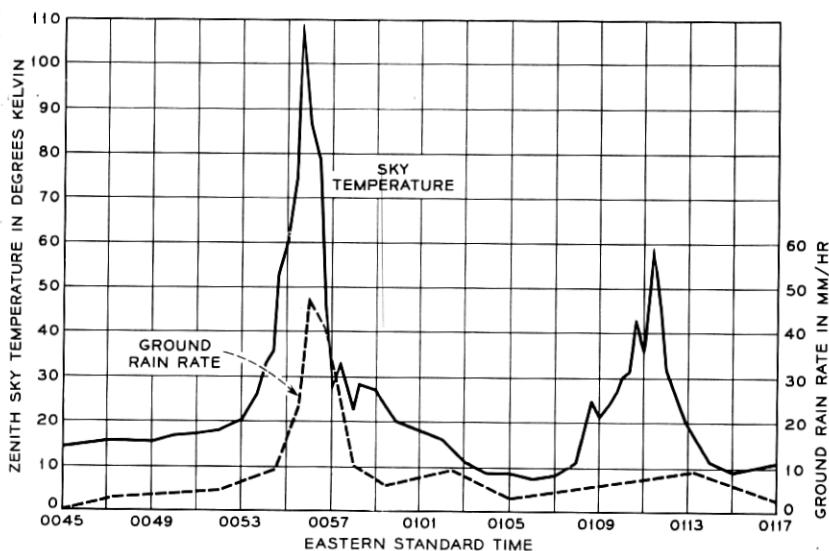


Fig. 11 — Example of lack of correlation between measured ground rain rate and zenith sky noise temperature (data of June 18, 1960). Compare these data with those in Fig. 8.

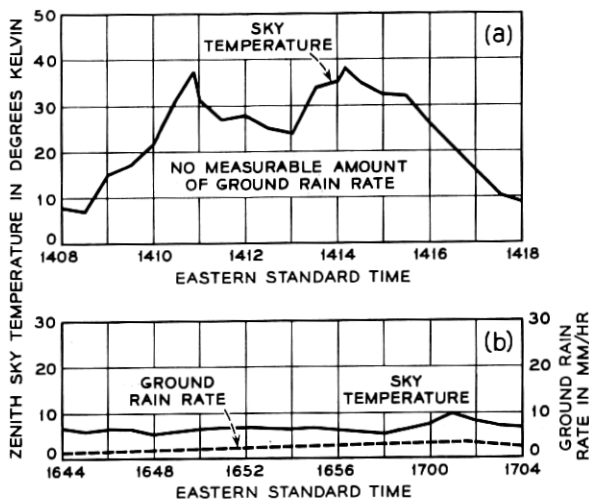


Fig. 12 — (a) Example of lack of correlation between measured ground rain rate and sky temperature (June 3, 1960); (b) small variations in sky noise temperature (July 27, 1960).

7.2 db above  $2.8^{\circ}\text{K}$ , the zenith temperature for an atmosphere containing a water vapor density of 10 grams per cubic meter, the corresponding median rain rate being 5 millimeters per hour. The noise temperature follows a log-normal distribution with a standard deviation of approximately 4 db. It should be cautioned that the relationships between the noise and rain rate distributions do not necessarily apply for any other general location, even though the ground rain rate distribution at that location is known.

It was mentioned in Section II that, if the distribution of rain along the antenna beam were known, one could calculate its noise contribution, since the absorption coefficient,  $\alpha$ , is a known function of wavelength and rain density. If the assumption is made that the raindrops are uniformly distributed over a given interval along the beam, then the absorption  $\alpha(r)$  is a constant over the interval. Calculations based upon (1), measured 6-kmc sky noise and measured ground rain rate, then can be made for the noise temperature which should obtain at other frequencies in the microwave band. For example, using this procedure,\* a

\* It should be noted that scattering of noise radiated from the earth into the antenna by the raindrops contributes to the total sky noise. However, calculations show that the scattering contribution is small. For example, again using a rainfall rate of 47.0 millimeters per hour and a measured 6 kmc temperature of  $110^{\circ}\text{K}$ , the contribution by scattering in the far field of the antenna is  $3.3^{\circ}\text{K}$ , the near field contribution  $0.6^{\circ}\text{K}$ , and the total scattered contribution  $3.9^{\circ}\text{K}$ , which is only 3.5 per cent of the total measured value.



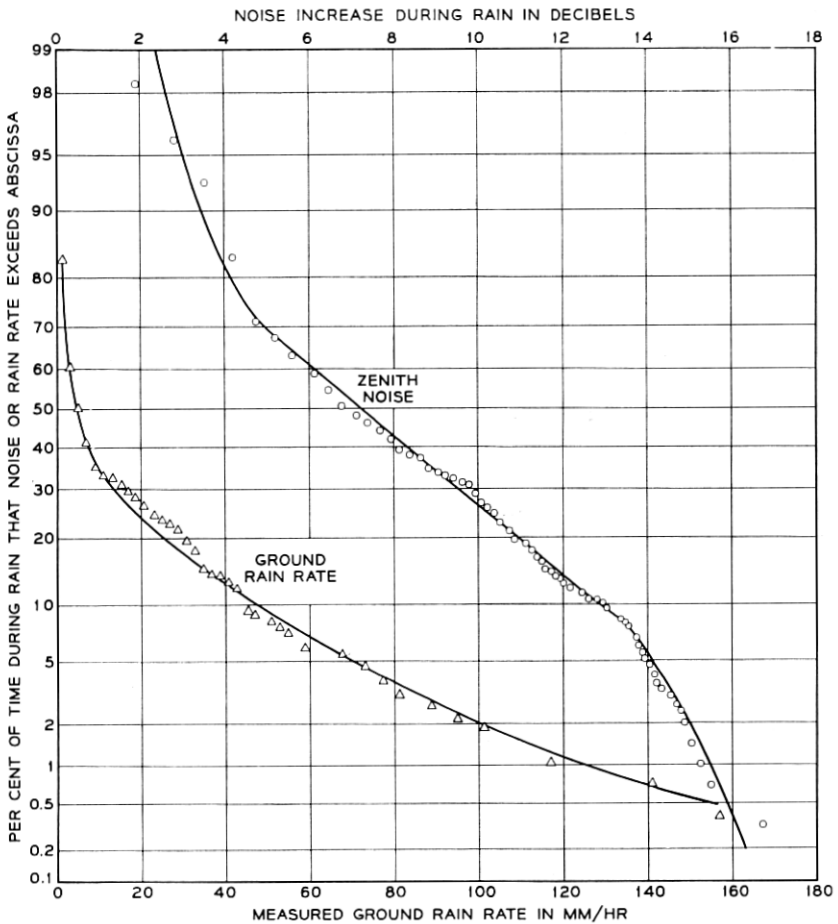


Fig. 13 — Percentage time distributions of zenith sky noise and ground rain rates, for eight rain periods from March 3, 1960 to July 27, 1960.

rainfall rate of 47.0 millimeters per hour that produced a measured temperature of  $110^{\circ}\text{K}$  at 6.0 kmc would produce a corresponding temperature of  $34^{\circ}\text{K}$  at 4.0 kmc, a decrease of 5.0 db.

Snow is another form of condensed water prevalent in the atmosphere. Noise measurements were made during a snowfall on January 27, 1961, but these show only a slight increase over those obtained on a clear day. Since snow is a fairly low-loss dielectric at centimeter wavelengths, this result is not unexpected.

## VI. CONCLUSIONS

Based upon measurements of sky noise temperatures made in atmospheres devoid of rain at a frequency of 6 kmc, the following seasonal changes in sky temperature can be expected: at an antenna beam position  $60^\circ$  from the zenith, approximately  $1\frac{1}{2}^\circ\text{K}$ ; at  $85^\circ$ , about  $15^\circ\text{K}$ . If the assumption is made that the desirable low-noise frequency band extends from 2 to 8 kmc, again neglecting the effects of rain, theoretical calculations establish the following limits: with an antenna beamed  $60^\circ$  from the zenith and for a frequency of 2 kmc, the seasonal change in sky temperature is  $0.6^\circ\text{K}$ ; for a frequency of 8 kmc, approximately  $5^\circ\text{K}$ . With an antenna beam  $85^\circ$  from the zenith at a frequency of 2 kmc, this change is  $1.0^\circ\text{K}$  and, at 8 kmc, it is  $26^\circ\text{K}$ . Data obtained at 6 kmc, with the antenna beam in the favorable zenith position, indicate that rain can increase the sky noise temperature as much as 17 db. In a space communication system, these changes in noise level are expected to play the counterpart of signal fading in line-of-sight communications; therefore suitable margins must be allowed for them.

## REFERENCES

1. Pierce, J. R., and Kompfner, R., Transoceanic Communications by Means of Satellites, Proc. I.R.E., **47**, 1959, p. 372; see also B.S.T.J., **40**, July, 1961, Project Echo issue.
2. Hogg, D. C., Effective Antenna Temperature Due to Oxygen and Water Vapor in the Atmosphere, J. Appl. Phys., **30**, 1959, p. 1417.
3. Tolbert, C. W., and Straiton, A. W., Anomalous Atmospheric Water Vapor Absorption of Millimeter Wavelength Radiation, U.R.S.I. meeting, fall 1960, Boulder, Colorado.
4. Gunn, K. L. S., and East, T. W. R., The Microwave Properties of Precipitation Particles, Quart. J. Roy. Meteor. Soc., **80**, 1954, p. 522.
5. DeGrasse, R. W., Hogg, D. C., Ohm, E. A., and Scovil, H. E. D., Ultra-Low-Noise Antenna and Receiver Combination for Satellite or Space Communication, Proc. Nat. Elect. Conf., **15**, 1959, p. 370.
6. DeGrasse, R. W., Schulz-DuBois, E. O., and Scovil, H. E. D., The Three-Level Solid State Traveling-Wave Maser, B.S.T.J., **38**, 1959, p. 305.
7. Gunn, K. L. S., and Marshall, J. S., The Effect of Wind Shear on Falling Precipitation, J. Meteor., **12**, 1955, p. 339